01 Sep 2008

Intelligent Tool for Determining the True Harmonic Current Contribution of a Customer in a Power Distribution Network

Joy Mazumdar

Ronald G. Harley

Frank C. Lambert

Ganesh K. Venayagamoorthy
Missouri University of Science and Technology

et. al. For a complete list of authors, see https://scholarsmine.mst.edu/ele_comeng_facwork/1095

Intelligent Tool for Determining the True Harmonic Current Contribution of a Customer in a Power Distribution Network

Joy Mazumdar, *Member, IEEE*, Ronald G. Harley, *Fellow, IEEE*, Frank C. Lambert, *Senior Member, IEEE*, Ganesh Kumar Venayagamoorthy, *Senior Member, IEEE*, and Marty L. Page, *Member, IEEE*

***Abstract*—Customer loads connected to power distribution network may be broadly categorized as either linear or nonlinear. Nonlinear loads inject harmonics into the power network. Harmonics in a power system are classified as either load harmonics or as supply harmonics depending on their origin. The source impedance also impacts the harmonic current flowing in the network. Hence, any change in the source impedance is reflected in the harmonic spectrum of the current. This paper proposes a novel method based on artificial neural networks to isolate and evaluate the impact of the source impedance change without disrupting the operation of any load, by using actual field data. The test site chosen for this paper has a significant amount of triplen harmonics in the current. By processing the acquired data with the proposed algorithm, the actual load harmonic contribution of the customer is predicted. Experimental results confirm that attempting to predict the total harmonic distortion of a customer by simply measuring the customer's current may not be accurate. The main advantage of this method is that only waveforms of voltages and currents at the point of common coupling have to be measured. This method is applicable for both single- and three-phase loads.**

***Index Terms*—Harmonic analysis, neural networks, power quality, power system harmonics, total harmonic distortion (THD).**

I. Introduction

THE DEPENDENCE of modern life upon the continuous supply of electrical energy makes system reliability and power quality topics of utmost importance in the area of power system research. Modern day industrial applications extensively use power electronic devices. They have proven to be extremely useful, but, unfortunately, the current waveforms that these devices produce are not sinusoidal [1]. The presence of current and voltage harmonics in power distribution systems increases losses in lines, decreases the power factor, and can even cause resonance with capacitors connected in parallel to the system.

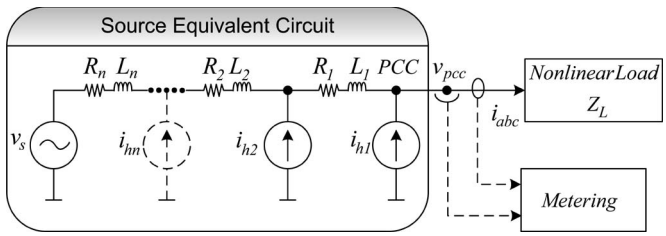

Fig. 1. Typical one-line diagram of a power distribution network.

Harmonics are an important measurable parameter of power quality. The related economic aspects of harmonics [2] and deregulation [3] have all created a need for extensive monitoring of the power system harmonics. Customers with sensitive equipment use harmonic current monitoring to locate the source of harmonic-related problems that might occur. On the other side, utilities try to meet the demands of their customers. They monitor the supply voltage to prove that the quality of the offered power is within the prespecified standards and to obtain the necessary information for solving problems [4].

Harmonic-related problems on electric utility distribution systems are usually created by primary metered customers. The significant harmonics are mostly 5th, 7th, 11th, and 13th with the 5th harmonic as the largest in most cases. Classic utility-side symptoms of harmonic problems are distorted voltage waveforms, blown shunt capacitor fuses, and transformer overheating. Capacitor losses are sensitive to harmonic voltages. Transformer losses are sensitive to harmonic currents.

A typical one-line diagram of a power distribution network is shown in Fig. 1. If the nonlinear load is supplied from a sinusoidal voltage source, its injected harmonic current $i_{\mathrm{abc}}(t)$ is referred to as *contributions from the load* or load harmonics. Harmonic currents cause harmonic volt drops in the supply network. Any other loads, even linear loads, connected to the point of common coupling (PCC) have harmonic currents injected into them by the distorted PCC voltage. Such currents are referred to as *contributions from the power system* or supply harmonics.

If several customers are connected to a PCC, it is not possible by traditional methods [5], [6] to accurately determine the

Paper MSDAD-07-70, presented at the 2006 Industry Applications Society Annual Meeting, Tampa, FL, October 8–12, and approved for publication in the IEEE TRANSACTIONS ON INDUSTRY APPLICATIONS by the Industrial Automation and Control Committee of the IEEE Industry Applications Society. Manuscript submitted for review October 31, 2006 and released for publication January 22, 2008. Current version published September 19, 2008. This work was supported by the National Electric Energy Testing Research and Applications Center (NEETRAC), Georgia Institute of Technology.

J. Mazumdar was with the School of Electrical Engineering, Georgia Institute of Technology, Atlanta, GA 30332-0250 USA. He is now with the Power Conversion Division, Siemens Energy and Automation, Alpharetta, GA 30005 USA (e-mail: joy.mazumdar@ieee.org).

R. G. Harley and F. C. Lambert are with the School of Electrical Engineering, Georgia Institute of Technology, Atlanta, GA 30332-0250 USA (e-mail: rharley@ece.gatech.edu).

G. K. Venayagamoorthy is with the Missouri University of Science and Technology, Rolla, MO 65409-0249 USA (e-mail: ganeshv@mst.edu).

M. L. Page is with Distribution Reliability and Management, Georgia Power Company, Atlanta, GA 30308-3374 USA (e-mail: malpage@southernco.com).

Color versions of one or more of the figures in this paper are available online at http://ieeexplore.ieee.org.

Digital Object Identifier 10.1109/TIA.2008.2002213

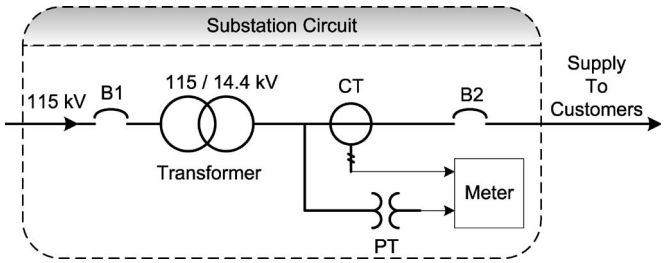

Fig. 2. Substation circuit and data acquisition schematic.

amount of harmonic current injected by each customer, in order to tell which customer(s) is injecting the excessively high harmonic currents, or whether the source is responsible for the harmonics by the virtue of a distorted PCC voltage. When measurements of current are taken at the PCC, it is expected that those measurements can be used to determine whether the customer is in compliance with IEEE 519 [7], [8]. However, results in this research show that the current measurements at the PCC are not always reliable. If there is a significant amount of distortion present in the PCC voltage, then this voltage distortion affects the current distortion measurements. This may create a situation that makes it appear as if a particular customer is not in compliance with the harmonic current limits because of the already distorted utility system voltage. In such a case, it may be necessary to determine what the customer's true current harmonic distortions would be if the PCC voltage could be a pure sinusoidal voltage.

However, establishing a pure sinusoidal voltage at the PCC may not be feasible since that would mean performing utility switching to reduce the system impedance to almost zero in order to get ν_s to appear at the PCC. An alternative approach is to use a neural network that is able to learn the customer's load admittance. Then, it is possible to predict the customer's true current harmonic distortions based on mathematically applying a pure sinusoidal voltage to the learned load admittance.

This paper addresses the issues related to the change of source impedance by a utility and how it impacts the power system network harmonics based on field data gathered at a substation in Georgia, USA. The test site chosen is primarily a residential feeder. Furthermore, this paper demonstrates the application of neural networks to predict the true harmonic current distortion of the customer under a specific resonance condition in the distribution system and validates the prediction when the utility changes the source impedance to remove the resonance condition.

II. Analysis of Acquired Data

The distribution system configuration at the measurement site is a three-phase four-wire system. The waveforms of phase A line-neutral voltage and the three line currents are acquired as six cycle snapshots, every 20 s, for a period of 2 1/2 h. Each snapshot measurement is designated as an event. Hence, 462 events are recorded. The sampling frequency for data acquisition is set at 256 samples per cycle. All data acquisition is done at the substation, as shown in Fig. 2. The measurement instrument acquires binary data files. The software import converts the data to text readable format.

A 20-A full-scale clamp on the current transformer (CT) is used, measuring only about 0.25 A in the relay circuit of the feeder breaker. The current therefore already reflects the CT ratios and represents the current in primary line values. The voltage is a 120-V measurement of a 25-kV line–line (14.4-kV line to neutral) service. Hence, a potential transformer (PT) ratio of 14400/120 is applied.

Fig. 3 shows the variation of the current THD for the three line currents over the entire period of measurement.

The THD values for the three line currents undergo a step change during event 238. This is the point when the utility switched some capacitor banks in the substation to effect a change in the source impedance. The phases A and B currents had THDs in the range of 10.5%–11% before the source impedance changed, and after the change, the THDs dropped to values between 8.5% and 9%. The phase C current THDs before and after the impedance change were 8% and 6.5%, respectively.

Fig. 4 shows the variation of the voltage THD for phase A over the entire period of measurement.

The voltage THD is well within the limits specified by IEEE 519 even after the small step increase when the impedance change is made.

Fig. 5 shows six cycles of the actual phase A voltage and current waveform acquired **before** the impedance change.

The voltage waveform in Fig. 5 appears clean, whereas the current waveform is extremely noisy. Noisy current waveforms with high harmonic content result in telephone interference, and the same was reported from this site. The Fourier spectrum of the current waveform in Fig. 5 is shown in Fig. 6 with a dominant 9th harmonic.

Fig. 7 shows six cycles of the phase A voltage and current waveforms **after** the impedance change. The current waveform in Fig. 7 is still noisy after the impedance change; however, the harmonic spectrum (Fig. 8) of the current has changed.

Some observations can be made from the aforementioned plots. There is a dc offset present in the current waveform, and the current is rich in high-frequency components. In particular, the 9th harmonic dominates and causes telephone interference on a street served by this feeder, which is the reason why this particular circuit is chosen for analysis. The aforementioned results indicate a possible network resonance. The switching in the substation changes the source impedance and causes a reduction in the 9th harmonic, as shown in Fig. 8. A high 9th harmonic is often the result of a single fuse blown on a three-phase capacitor bank, but in this case, no fuses were blown. However, there are some subdivision loads with underground service, and therefore, cable capacitance is present. Whatever may be the cause [9], the customer current has triplen harmonics, and the customer could be held responsible to take corrective actions to rectify the same [10], [11], unless it could be proven that these triplen harmonics cannot be attributed to the customer.

III. Estimation of Harmonic Current

Artificial neural networks (ANNs) have provided an alternative modeling approach for power system applications. The

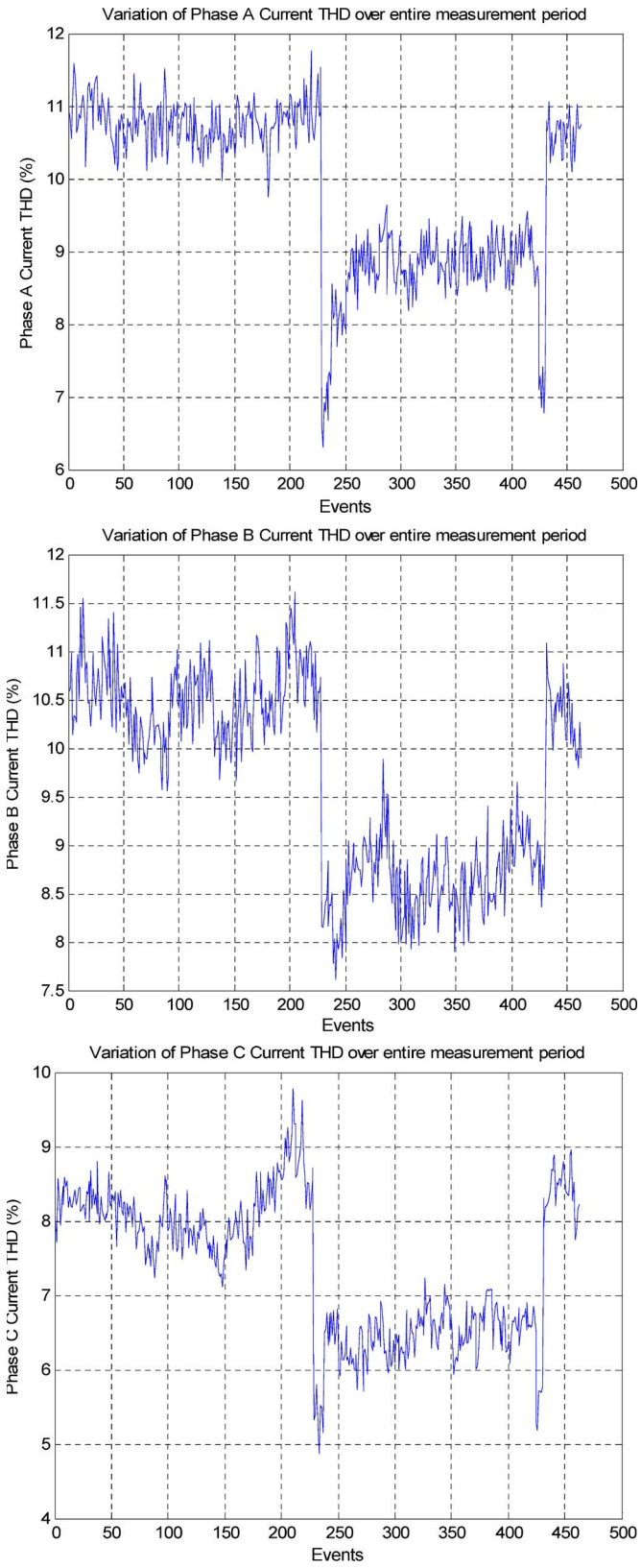

Fig. 3. Variation of current THD for the three line currents.

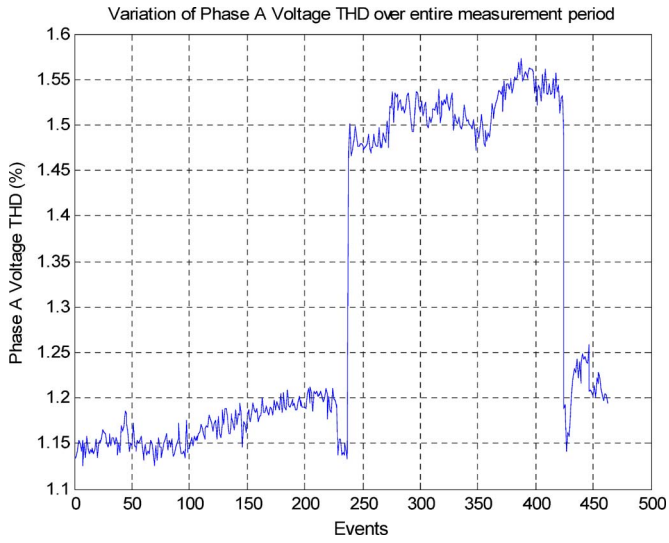

Fig. 4. Variation of phase A voltage THD.

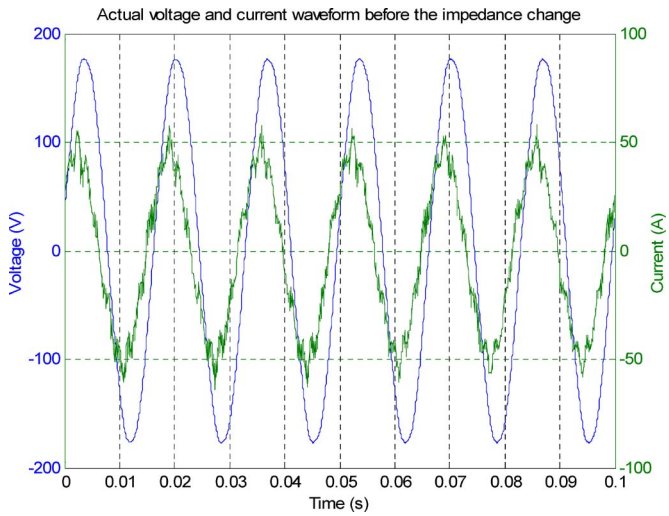

Fig. 5. Six cycles of acquired voltage and current waveform before the impedance change.

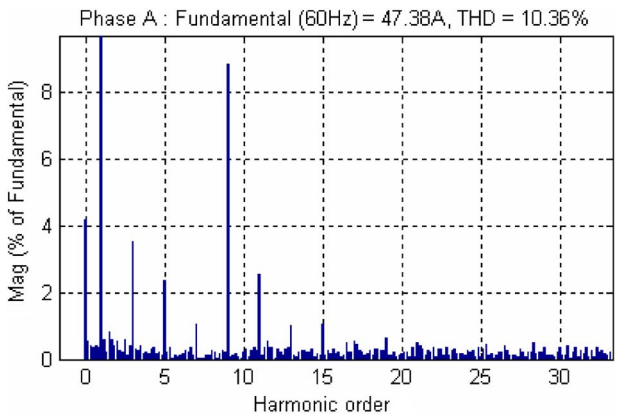

Fig. 6. FFT plot of phase A current before source impedance change.

multilayer perceptron network (MLPN) is one of the most popular topologies in use today [12]. This paper uses a method based on MLPN to predict the true harmonic current distortion that can be attributed to a customer, without disrupting the operation of any customer. The method was originally proposed in [13] and [14]. A single-line diagram, consisting of

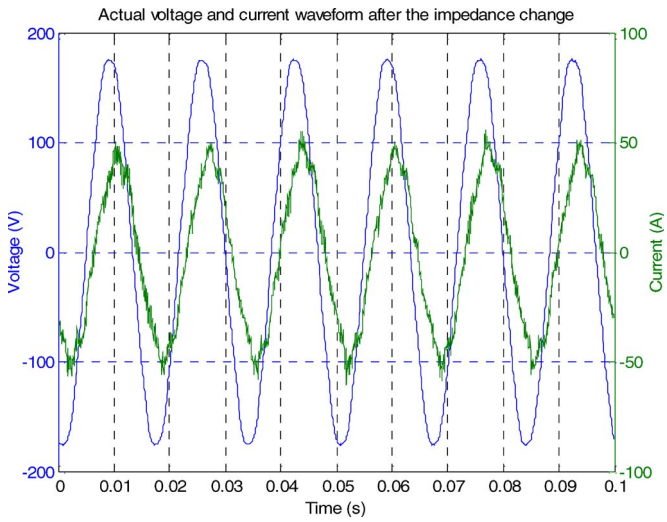

Fig. 7. Six cycles of acquired voltage and current waveform after the impedance change.

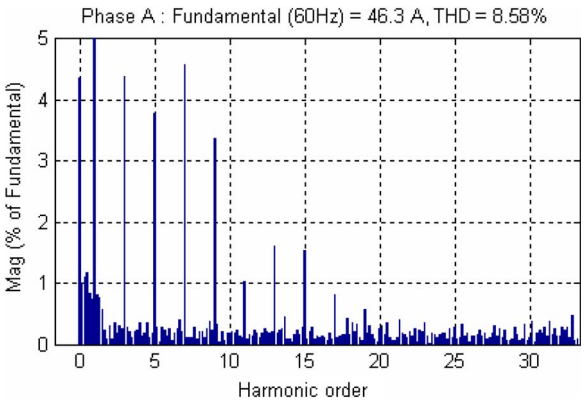

Fig. 8. FFT plot of phase A current after source impedance change.

the utility equivalent circuit, the customer, and the neural-network-based load model identifier (LMI), is shown in Fig. 9. The utility equivalent circuit is composed of a three-phase supply network having a sinusoidal voltage source $\nu_{\rm s}$, network impedance $L_{\rm s}$, $R_{\rm s}$, and several other loads, which can be linear or nonlinear.

The LMI consists of two individual neural network blocks, namely, the **identification** neural network (ANN1) and the **estimation** neural network (ANN2). The voltage $\nu_{\rm abc}$ and the current $i_{\rm abc}$ at the service entrance of the customer are the parameters of interest and are processed by the LMI.

A. Brief Description of the Scheme

The customer's load currents $i_{\rm a}$, $i_{\rm b}$, and $i_{\rm c}$ (denoted by $i_{\rm abc}$) are composed of load harmonics as well as supply harmonics. However, the utility sees the line current $i_{\rm abc}$ as the harmonic distortion injected into the network by the load. ANN1 is trained to **identify** the nonlinear characteristics of the load (in the case of a single-phase load), and for each phase individually for a three-phase load. At any moment in time after the ANN1 training has been completed, its weights are transferred to ANN2. ANN2 is then supplied offline with a three-phase

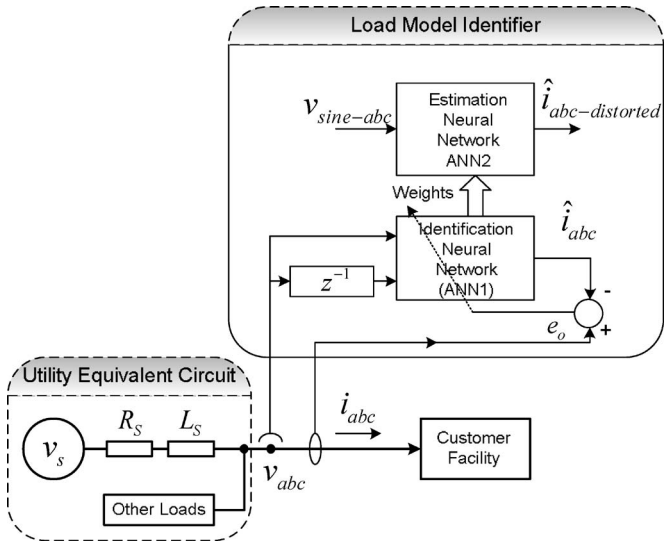

Fig. 9. Harmonic current prediction scheme.

mathematically generated sine wave $\nu_{\rm sine\text{-}abc}$ to estimate its three output currents $\hat{i}_{\rm abc\text{-}distorted}$. Any distortion present in the current waveforms $\hat{i}_{\rm abc\text{-}distorted}$ can now truly be attributed to the nonlinearity of the load admittance. This procedure is known as load modeling. ANN2 is a replica of the trained ANN1 structurally. The function of ANN2 could have been carried out by ANN1, but that would disrupt the continual online training of ANN1 during the brief moments when $\hat{i}_{\rm abc\text{-}distorted}$ has to be estimated. The algorithms of ANN1 and ANN2 are executed in software.

B. Operation of the ANN1

The proposed method measures the instantaneous values of the three voltages $\nu_{\rm abc}$ at the PCC, as well as the three line currents $i_{\rm abc}$ at the kth moment in time. The voltages $\nu_{\rm abc}$ could be line-to-line or line-to-neutral measurements. The ANN1 is designed to predict one step ahead the line current $\hat{i}_{\rm abc}$ as a function of the present and delayed voltage vector values $\nu_{\rm abc}(k)$, $\nu_{\rm abc}(k-1)$, and $\nu_{\rm abc}(k-2)$. When the $(k+1)$th moment arrives (at the next sampling instant), the actual measured instantaneous values of $i_{\rm abc}$ are compared with the previously predicted values of $\hat{i}_{\rm abc}$, and the error $e_{\rm o}$ is used to train the ANN1 weights. This ensures continual online training of ANN1.

Initially, the weights have random values, but after several sampling steps, the training soon converges, and the value of the error $e_{\rm o}$ in Fig. 9 diminishes to an acceptably small value, as expressed by the value of mean squared error (mse) in (8). Proof of this is illustrated by the fact that the individual phase waveforms for $i_{\rm abc}$ and $\hat{i}_{\rm abc}$ should practically lie on top of each other, respectively. At this point, the ANN1 therefore represents the admittance of the nonlinear load. This process is called identifying the load admittance. Since continual online training is used, it will correctly represent the load admittance from moment to moment. At any moment in time after the ANN1 training has converged, its weights are transferred to ANN2. The training cycle of ANN1 continues to follow load changes,

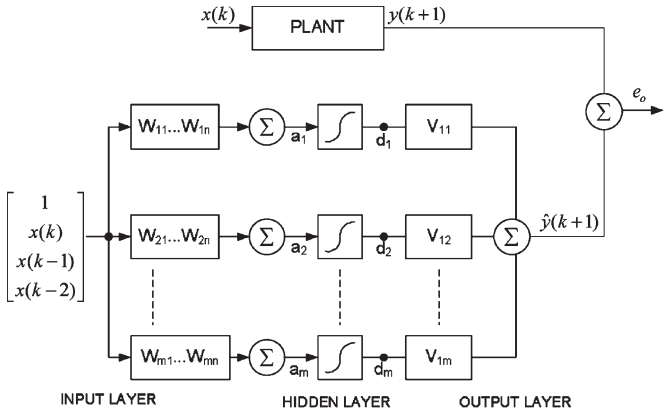

Fig. 10. Structure of an MLPN.

and in this way, ANN2 always has updated weights available when needed.

C. Operation of the ANN2

The ANN2 is supplied with a mathematically generated sine wave to estimate its output. The output of ANN2 called $\hat{i}_{\text{abc-distorted}}$ therefore represents the current that the nonlinear load would have drawn had it been supplied by a sinusoidal voltage source. Any distortion present in $\hat{i}_{\text{abc-distorted}}$ can now truly be attributed to the nonlinearity of the load admittance.

Once a number of $\hat{i}_{\text{abc-distorted}}$ cycles have been calculated by ANN2, they are stored (and subsequently used for harmonic analysis to find the true load-injected current total harmonic distortion THD$_i$). New weights are then uploaded from ANN1 to ANN2, and a series of new $\hat{i}_{\text{abc-distorted}}$ cycles and a new THD$_i$ are calculated. This THD$_i$ value may be recorded or displayed at frequent predetermined intervals, or an average value calculated over a period of time.

Due to the nature of the sigmoidal transfer function, the outputs of the neurons in the hidden layer are limited to values between zero and one. The inputs to the neural networks are therefore first scaled to fall within the limits of ± 1.The scaling of the acquired data is done using software, and hence, that removes any limitations whatsoever on the data acquisition system and the transducers.

D. ANN Governing Equations

The structure of an MLPN is shown in Fig. 10. This network consists of a set of input neurons, output neurons, and one or more hidden layers of intermediate neurons. Data flow into the network through the input layer, pass through the hidden layer, and finally flow out of the network through the output layer. The network thus has a simple interpretation as a form of input–output model, with weights as free parameters [15].

The process of passing the inputs in Fig. 10 through the neural network structure to its output is known as forward propagation. Every input in the input column vector $\underline{x}$ is fed via the corresponding weight in the input weight matrix W to every node in the hidden layer to determine the activation vector $\underline{a}$. Each of the hidden neuron activations in $\underline{a}$ is then passed through a sigmoidal function to determine the hidden-layer decision vector $\underline{d}$-

$$\underline{a} = W\underline{x} \tag{1}$$

$$d_i = \frac{1}{1+e^{(-a_i)}}, \qquad i \in \{1, 2, \ldots, m\} \tag{2}$$

where $\underline{x} \in R^n$ is the input column vector, $\underline{a} \in R^m$ is the hidden-layer activation column vector, $W \in R^{m\times n}$ is the input weight matrix, n is the number of inputs to the ANN, including the bias, and m is the number of neurons in the hidden layer. The elements of the decision vector $\underline{d}$ are then fed to the corresponding weight in the output weight matrix V.

The ANN output is computed as

$$\hat{y} = (V\underline{d})^{\mathrm{T}}. \tag{3}$$

For a single output system, the output weight matrix $V \in R^{1\times m}$ and $\hat{y}$ is a scalar.

The output error is calculated as

$$e_{\mathrm{o}} = y - \hat{y}. \tag{4}$$

The process of passing the output error to the input in order to estimate the individual contribution of each weight in the network to the final output error is known as error backpropagation. The weights are then modified so as to reduce the output error. The change in input weights ΔW and output weights ΔV at step k are calculated as

$$\begin{aligned} \Delta W(k) &= \gamma_{\mathrm{m}}\Delta W(k-1) + \gamma_{\mathrm{g}}\underline{e}_a\underline{x}^{\mathrm{T}} \\ \Delta V(k) &= \gamma_{\mathrm{m}}\Delta V + \gamma_{\mathrm{g}}\underline{e}_y\underline{d}^{\mathrm{T}} \end{aligned} \tag{5}$$

where γ_{m}, $\gamma_{\mathrm{g}} \in [0, 1]$ are the momentum and learning gain constants, respectively. The last step in the training process is the actual updating of the weights at step k

$$\begin{aligned} W(k) &= W(k-1) + \Delta W(k) \\ V(k) &= V(k-1) + \Delta V(k). \end{aligned} \tag{6}$$

E. Selection of Optimal Number of Neurons for Hidden Layer

To model the harmonic characteristics of a nonlinear load, the ANN architecture needs to address the issues regarding the following:

1) the number of layers;
2) the number of neurons in each layer;
3) the hidden-layer activation function.

For any nonlinear function identification type problem, at least one hidden layer is required. Additionally, a nonlinear continuously differentiable hidden-layer activation function, such as the sigmoidal function, allows the network to perform nonlinear modeling. Depending on the application, the number of ANN inputs and the number of outputs are fixed. The only structural variable then remaining is the number of neurons m in the hidden layer. The ANN execution time and the training convergence are directly dependent on the value of m. Two performance criteria for the measure of ANN training convergence

are typically used; they are the absolute value of the tracking error T_{e} defined as

$$T_{\mathrm{e}} = |(y - \hat{y})| \tag{7}$$

and the mse defined as

$$\mathrm{mse} = \frac{1}{r}\sum_{1}^{r} |(y - \hat{y})|^2 \tag{8}$$

where r is the number of training epochs. The tracking error T_{e} varies at a high rate as training progresses. For this reason, it is more convenient to consider the mse which is a smooth curve due to the averaging process. In neural network training, it is not possible to get the mse to be exactly zero; thus, the objective is to get it down below some minimum value, typically $(\mathrm{mse}_{\min} < 10^{-2})$. This can be achieved by providing information to the neural network about the history of the system dynamics, typically in the form of delayed inputs and outputs.

The number of neurons in the hidden layer affects the rate and the final value of the mse convergence, and is typically chosen on a heuristic basis after several iterations. For the specific problem presented in this paper, based on experimental data and experience, the following formula provides a starting point for choosing the number of neurons in the hidden layer:

$$H_{\mathrm{n}} \approx \frac{K * n}{C \cdot S \cdot \mathrm{mse}_{\min}} \tag{9}$$

where H_{n} is the number of neurons in the hidden layer, C is the number of cycles of training data, $\mathrm{mse}_{\min}$ is the acceptable mse in training, S is the number of samples per cycle of the acquired data, n is the number of inputs, and K is a constant depending on the number of inputs used and the sampling frequency of data. The aforementioned formula has been adapted from the work of Baum and Haussler [16].

The data acquisition meter used at the site is an AVO Megger PA-9 Plus meter with data sampling set at 256 samples/cycle. Starting with random initial values for the ANN weights, and to achieve an $\mathrm{mse}_{\min}$ of 0.2% with data from one event (i.e., six cycles), the value of K comes out to be 24. By substituting these values in (9), the value of H_{n} is 23. Fig. 11 shows the value of mse for ANN1 obtained experimentally for different values of neurons in the hidden layer. For the work presented in this paper, the number of neurons used in the hidden layer is 20.

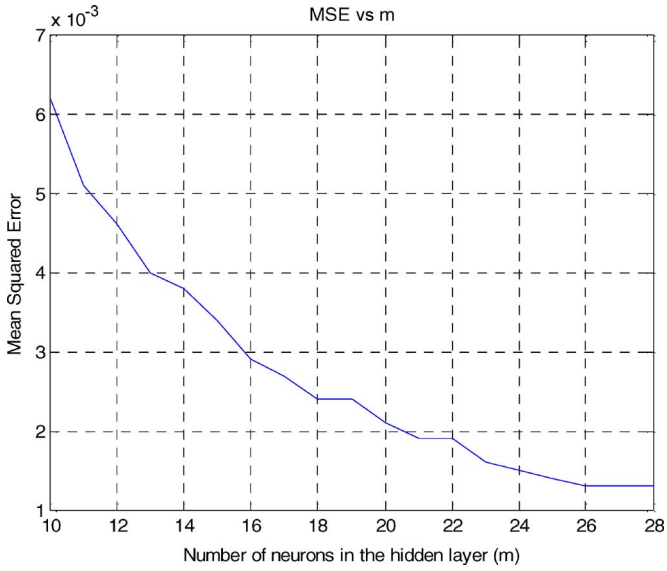

Fig. 11. Variation of mse over different values of the number of neurons in the hidden layer for ANN1.

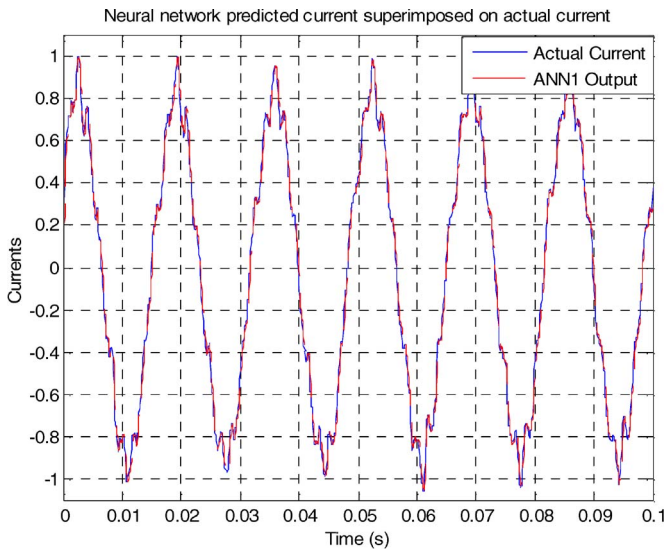

Fig. 12. Demonstration of ANN1 training: waveforms of i_{a} and $\hat{i}_{\mathrm{a}}$ coincide.

IV. Experimental Results

A. Before Source Impedance Change

The method of using online-trained ANNs to identify the load admittance and utilizing the trained neural network to estimate the true harmonic current injection of a customer is demonstrated with the help of field data.

The text readable field data from the AVO Megger PA-9 Plus meter are imported to MATLAB and passed on to the neural network code. The powergui block of Simulink is used to calculate the voltage and current THDs. These THDs are then compared with the values computed directly by the field instrument, in order to verify that both the values are the same.

The phase A voltage and current data in Fig. 4 are used as the pilot data since that has the highest 9th order harmonic and also has the highest harmonic current distortion. These data are passed through a second-order low-pass filter (implemented in Simulink) with cutoff frequency $f_{\mathrm{c}} = 2$ kHz in order to eliminate the high-frequency components. The conditioned data are used to train the neural network ANN1 until the training error converges to near zero, and the output of ANN1 $\hat{i}_{\mathrm{a}}$ correctly tracks the actual phase A current i_{a} of the customer. Fig. 12 shows how well ANN1 has converged since its output $\hat{i}_{\mathrm{a}}$ coincides with the actual i_{a} waveform.

The convergence of the training can also be verified by considering the mse in Fig. 13 which has a value less than 10^{-2} and almost constant after 400 epochs.

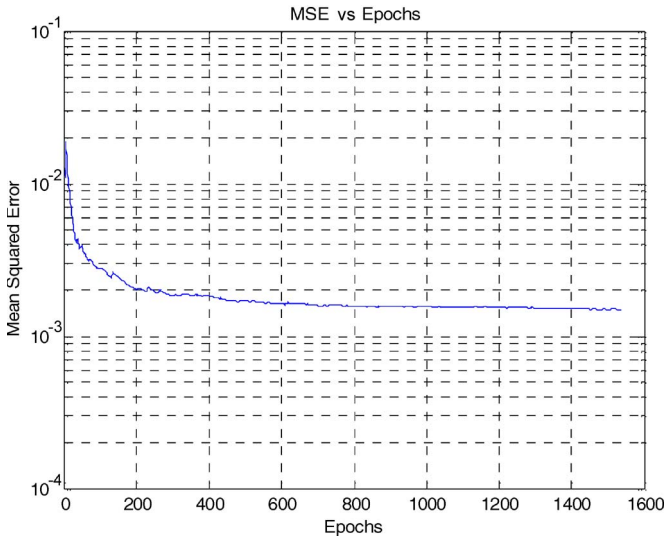

Fig. 13. Measure of ANN1 training convergence: mse in current training.

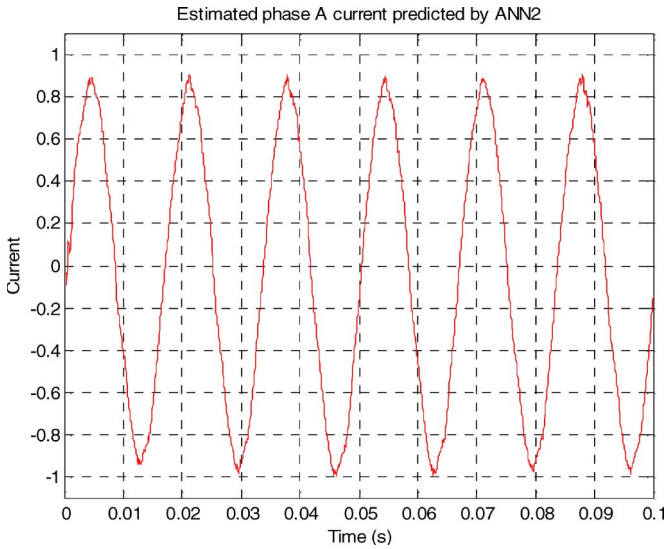

Fig. 14. Estimated phase A current when supplied with clean sine wave.

Once the training error is below a predefined level $\text{mse}_{\min}$ ($< 10^{-2}$), it can be concluded that ANN1 has learned the admittance of the customer load to an acceptable level of accuracy. The weights of ANN1 are now transferred to ANN2. While the ANN1 training continues, the computations of ANN2 are done offline.

ANN2 is now supplied with a mathematically generated sine-wave voltage with zero distortion as its input. This is equivalent to the situation wherein the customer is getting a clean sine-wave voltage at its service entrance and the resonance point in the line, along with other disturbances and supply harmonics, is being avoided. Any load serviced by a utility is designed and optimized to operate at 60 Hz; however, once it is connected to the power system network, it rarely receives a clean 60-Hz supply. The output of ANN2 is $\hat{i}_{\text{a-distorted}}$ and is shown in Fig. 14.

In other words, the $\hat{i}_{\text{a-distorted}}$ waveform gives the same information that could have been obtained by quickly removing the customer from the line (if this were possible) and connecting a pure sinusoidal voltage source to the service entrance of the customer, except that it is not necessary to actually do this interruption. The frequency spectrum of the $\hat{i}_{\text{a-distorted}}$ waveform is shown in Fig. 15.

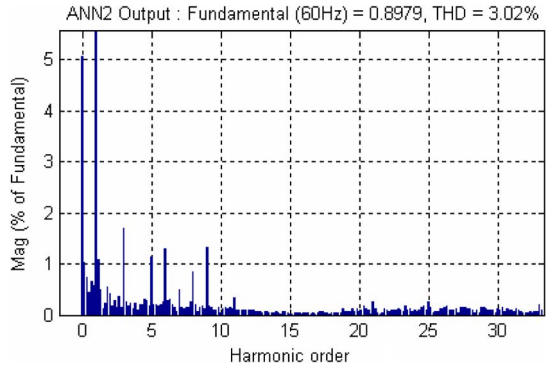

Fig. 15. FFT spectrum of the ANN2 predicted current waveform.

The true current distortion of the customer turns out to be **3.02%** in Fig. 15 instead of the **10.36%** of Fig. 6. However, a more significant finding from the fast Fourier transform (FFT) spectrum is the reduction of the 9th harmonic from **8.5%** to about **1.5%** of the fundamental.

B. After Source Impedance Change

The source impedance switching by the utility detunes the resonance point in the feeder, and that results in the reduction of the 9th harmonic from **8.5%** to about **3.5%** of the fundamental, as shown in Fig. 8. This result does show that for the particular operating point of the feeder, a resonance condition has a detrimental effect on the power distribution network and triggers the 9th harmonic in the customer's current.

Application of the load modeling tool shows that the 9th harmonic current is caused by both the customer and the utility and not just by the customer alone.

V. Conclusion

If individual harmonic current injections were known, then a utility could penalize the offending customer in some appropriate way, including, for example, a special tariff or insist on corrective action by the customer. Simply measuring the harmonic currents for each individual customer is not sufficiently accurate since these harmonic currents may be caused by not only the nonlinear load but also by a nonsinusoidal PCC voltage.

This paper demonstrated the ability of MLPNs to learn the admittance of the customer load using actual field data and utilize a trained neural network for estimating the true harmonic distortion caused by that customer. The advantages of this method are that it can be implemented online without disrupting the operation of any load, since only voltages and currents need to be measured; it does not require any special instruments, and it does not need to make any assumptions about any quantities, e.g., the impedance of the source, or a sine-wave PCC voltage. Every customer has individual power meters which are already receiving the waveforms of voltage and currents, and hence, it is a feasible option to implement the scheme for each customer individually.

Standards like IEEE 519 provide guidelines for regulating harmonic distortion levels that divide the responsibility between the utility and the customer. The utility has to maintain voltage distortion at the PCC below the specified limits, and the customer has to limit the amount of harmonic current injection onto the utility system. However, when certain unusual events like resonance occur in a power system, for instance, the load modeling tool provides a starting point for the troubleshooting to detect the origin of the problem. The information provided by the new method regarding the true current distortion of a load could be used to persuade an offending customer to take steps to mitigate an unacceptably high level of distortion.

The load modeling tool is designed in software and, hence, can be integrated into any existing power quality diagnostic instrument or be fabricated as a stand-alone instrument that could be installed in substations of large customer loads or used as a hand-held clip on instrument.

ACKNOWLEDGMENT

The authors would like to thank the Georgia Power Company for providing the field data and technical assistance required for this paper.

REFERENCES

[1] E. L. Owen, "A history of harmonics in power systems," *IEEE Ind. Appl. Mag.*, vol. 4, no. 1, pp. 6–12, Jan./Feb. 1998.
[2] M. F. McGranaghan, "Economic evaluation of power quality," *IEEE Power Eng. Rev.*, vol. 22, no. 2, pp. 8–12, Feb. 2002.
[3] J. Arrillaga, M. H. J. Bollen, and N. R. Watson, "Power quality following deregulation," *Proc. IEEE*, vol. 88, no. 2, pp. 246–261, Feb. 2000.
[4] Y. H. Yan, C. S. Chen, C. S. Moo, and C. T. Hsu, "Harmonic analysis for industrial customers," *IEEE Trans. Ind. Appl.*, vol. 30, no. 2, pp. 462–468, Mar./Apr. 1994.
[5] W. Xu and Y. Liu, "A method for determining customer and utility harmonic contributions at the point of common coupling," *IEEE Trans. Power Del.*, vol. 15, no. 2, pp. 804–811, Apr. 2000.
[6] K. Srinivasan, "On separating customer and supply side harmonic contributions," *IEEE Trans. Power Del.*, vol. 11, no. 2, pp. 1003–1012, Apr. 1996.
[7] *IEEE Recommended Practices and Requirements for Harmonic Control in Electric Power Systems*, IEEE Std. 519-1992, 1992.
[8] T. M. Blooming and D. J. Carnovale, "Harmonic convergence," *IEEE Ind. Appl. Mag.*, vol. 13, no. 1, pp. 21–27, Jan./Feb. 2007.
[9] Z. Huang, W. Xu, and V. R. Dinavahi, "A practical harmonic resonance guideline for shunt capacitor applications," *IEEE Trans. Power Del.*, vol. 18, no. 4, pp. 1382–1387, Oct. 2003.
[10] H. Fujita and H. Akagi, "A practical approach to harmonic compensation in power systems—Series connection of passive and active filters," *IEEE Trans. Ind. Appl.*, vol. 27, no. 6, pp. 1020–1025, Nov./Dec. 1991.
[11] P.-T. Cheng, S. Bhattacharya, and D. Divan, "Operations of the dominant harmonic active filter (DHAF) under realistic utility conditions," *IEEE Trans. Ind. Appl.*, vol. 37, no. 4, pp. 1037–1044, Jul./Aug. 2001.
[12] B. Burton and R. G. Harley, "Reducing the computational demands of continually online-trained artificial neural networks for system identification and control of fast processes," *IEEE Trans. Ind. Appl.*, vol. 34, no. 3, pp. 589–596, May/Jun. 1998.
[13] R. Harley, F. Lambert, T. Habetler, and J. Mazumdar, "System and method for determining harmonic contributions from nonlinear loads," U.S. Patent 7 013 227, Mar. 14, 2006.
[14] J. Mazumdar, R. Harley, and F. Lambert, "System and method for determining harmonic contributions from non-linear loads," in *Conf. Rec. IEEE IAS Annu. Meeting*, Hong Kong, Oct. 2–6, 2005, vol. 4, pp. 2456–2463.
[15] S. Haykin, *Neural Networks—A Comprehensive Foundation*, 2nd ed. Englewood Cliffs, NJ: Prentice-Hall, 1998.
[16] E. B. Baum and D. Haussler, "What size net gives valid generalization?" *Neural Comput.,* vol. 1, no. 5, pp. 151–160, Spring 1989.

Joy Mazumdar (S'00–M'06) received the B.S. degree in electronics engineering from Shivaji University, Kolhapur, India, in 1994, the M.S. degree in electrical engineering from the University of Central Florida, Orlando, in 2002, and the Ph.D. degree in electrical engineering from the Georgia Institute of Technology, Atlanta, in 2006.

He is currently with the Siemens Energy and Automation, Power Conversion Division, Alpharetta, GA, as a Senior Systems Engineer. Prior to graduate school, he was a Power Electronics Engineer with Siemens, Ltd., India, from 1995 to 2000. His current responsibilities include design and new application development for active front ends, power system studies leading to utility compliance, and utility-scale energy storage. His other research focuses on the development of a power system harmonics monitoring tool using neural network techniques. He is the joint holder of two patents, one issued and one pending. His research interests include utility applications of power electronics, power quality issues, active filters, inverter design for renewable energy systems, switching power supplies, variable-speed drives, and control techniques.

Ronald G. Harley (M'77–SM'86–F'92) received the M.Sc.Eng. degree in electrical engineering (*cum laude*) from the University of Pretoria, Pretoria, South Africa, in 1965, and the Ph.D. degree from London University, London, U.K., in 1969.

In 1971, he was appointed as the Chair of Electrical Machines and Power Systems, University of Natal, Durban, South Africa, where he was a Professor of electrical engineering for many years and became the Department Head and the Deputy Dean of Engineering. He is currently the Duke Power Company Distinguished Professor with the School of Electrical Engineering, Georgia Institute of Technology, Atlanta. He has coauthored some 380 papers in refereed journals and international conference proceedings. He is the holder of three patents. His research interests include dynamic behavior and condition monitoring of electric machines, motor drives, power systems and their components, and controlling them by the use of power electronics and intelligent control algorithms.

Dr. Harley is a Fellow of the Institution of Electrical Engineers, U.K. He is also a Fellow of the Royal Society in South Africa and a Founder Member of the Academy of Science in South Africa formed in 1994. During 2000 and 2001, he was one of the IEEE Industry Applications Society's six Distinguished Lecturers. He was the Vice-President of Operations of the IEEE Power Electronics Society from 2003 to 2004 and the Chair of the Atlanta Chapter of the IEEE Power Engineering Society. He is currently the Chair of the Distinguished Lecturers and Regional Speakers program of the IEEE Industry Applications Society. He was the recipient of the Cyrill Veinott Award in 2005 from the IEEE Power Engineering Society for his "outstanding contributions to the field of electromechanical energy conversion." Ten of his coauthored papers have also attracted prizes from journals and conferences.

Frank C. Lambert (SM'90) received the B.S. and M.S. degrees in electric power engineering from the Georgia Institute of Technology (Georgia Tech), Atlanta, in 1973 and 1976, respectively.

From 1973 to 1995, he was with the Georgia Power Company, gaining experience in distribution and transmission engineering, operations, and management. He worked with Georgia Tech to develop a graduate course in high-voltage engineering and cotaught the laboratory sessions. He joined the National Electric Energy Testing Research and Applications Center (NEETRAC) in 1996 to manage the Electrical Systems Research Program and is active in PES, where he serves on several working groups in the Distribution Subcommittee. He is currently the Electrical Systems Program Manager with NEETRAC, School of Electrical Engineering, Georgia Tech.

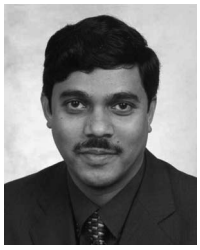

Ganesh Kumar Venayagamoorthy (S'91–M'97–SM'02) received the B.Eng. (Honors) degree in electrical and electronics engineering (with a first class honors) from the Abubakar Tafawa Balewa University, Bauchi, Nigeria, in 1994, and the M.Sc.Eng. and Ph.D. degrees in electrical engineering from the University of Natal, Durban, South Africa, in 1999 and 2002, respectively.

He is currently an Associate Professor of electrical and computer engineering and the Director of the Real-Time Power and Intelligent Systems Laboratory, Missouri University of Science and Technology, Rolla. His research interests include power systems stability and control, computational intelligence, signal processing, and evolvable hardware. He has published about 200 papers in refereed journals and international conference proceedings.

Dr. Venayagamoorthy is currently the Chapter Chair of the IEEE St. Louis CIS and IAS, the Chair of the Task Force on Intelligent Control Systems and the Secretary of the Intelligent Systems subcommittee of the IEEE Power Engineering Society, and the Chair of the IEEE CIS Task Force on Power System Applications. He was the recipient of the following awards: the 2005 IEEE Industry Applications Society (IAS) Outstanding Young Member Award, the 2005 South African Institute of Electrical Engineers Young Achievers Award, the 2004 IEEE St. Louis Section Outstanding Young Engineer Award, the 2003 International Neural Network Society Young Investigator Award, the 2001 IEEE Computational Intelligence Society (CIS) Walter Karplus Summer Research Award, and five prize papers from the IEEE IAS and the IEEE CIS.

Marty L. Page (M'04) was born in Dalton, GA, in 1959. He received the B.S. degree in electrical engineering technology from Southern Polytechnic Institute, Marietta, GA, in 1982.

He has been with the Georgia Power Company, Atlanta, working in various engineering positions throughout his entire career, where he is currently with Distribution Reliability and Management. He has experience in transmission system fault data acquisition and analysis, substation testing and commissioning, power quality investigations within industrial and commercial facilities, and distribution system power quality management.

Mr. Page is a member of the IEEE Power Engineering Society. He is a Registered Professional Engineer in the State of Georgia.